Research Article | Vol. 7, No. 12 | 1 Dec 2017 | OPTICAL MATERIALS EXPRESS 4367
Optical Materials EXPRESS

Recombination dynamics in $CsPbBr_3$ nanocrystals: role of surface states

FABIO GABELLONI,[1] FRANCESCO BICCARI,[1,*] GIULIA ANDREOTTI,[1] DARIO BALESTRI,[1] SIMONA CHECCUCCI,[1] ALESSIO MILANESI,[2] NICOLA CALISI,[2] STEFANO CAPORALI,[3,4] AND ANNA VINATTIERI[1]

[1] *Department of Physics and Astronomy – LENS, University of Florence, via G. Sansone 1, I-50019 Sesto Fiorentino (FI), Italy*
[2] *Department of Chemistry, University of Florence, via della Lastruccia 3, I-50019 Sesto Fiorentino (FI), Italy*
[3] *Department of Industrial Engineering DIEF, University of Florence, via S. Marta 3, I-50139 Firenze, Italy*
[4] *Consiglio Nazionale delle Ricerche-Istituto dei Sistemi Complessi CNR-ISC, Via Madonna del Piano 10, I-50019 Sesto Fiorentino (FI), Italy*
[*] *francesco.biccari@unifi.it*

Abstract: We present a detailed experimental investigation of the carrier recombination dynamics in $CsPbBr_3$ films by means of picosecond time-resolved photoluminescence. Temperature-dependent measurements show that carrier capture and release from the nanocrystals (NCs) surfaces determine the observed increase of the recombination lifetime with the increase of temperature. This result opens the way to probe the surface of the NCs, which is of the utmost relevance for optoelectronic applications, and to eventually give feedback for surface treatments of NCs.

OCIS codes: : (160.4236) Nanomaterials; (160.6000) Semiconductor materials; (250.5230) Photoluminescence.

References and links

1. Y.-H. Kim, H. Cho, and T.-W. Lee, "Metal halide perovskite light emitters," PNAS **113**, 11694–11702 (2016).
2. X. Li, F. Cao, D. Yu, J. Chen, Z. Sun, Y. Shen, Y. Zhu, L. Wang, Y. Wei, Y. Wu, and H. Zeng, "All inorganic halide perovskites nanosystem: Synthesis, structural features, optical properties and optoelectronic applications," Small **13**, 1603996 (2017).
3. L. Protesescu, S. Yakunin, M. I. Bodnarchuk, F. Krieg, R. Caputo, C. H. Hendon, R. X. Yang, A. Walsh, and M. V. Kovalenko, "Nanocrystals of cesium lead halide perovskites ($CsPbX_3$, X = Cl, Br, and I): Novel optoelectronic materials showing bright emission with wide color gamut," Nano Lett. **15**, 3692–3696 (2015).
4. M. Kulbak, S. Gupta, N. Kedem, I. Levine, T. Bendikov, G. Hodes, and D. Cahen, "Cesium enhances long-term stability of lead bromide perovskite-based solar cells," J. Phys. Chem. Lett. **7**, 167–172 (2016).
5. X. Du, G. Wu, J. Cheng, H. Dang, K. Ma, Y.-W. Zhang, P.-F. Tan, and S. Chen, "High-quality $CsPbBr_3$ perovskite nanocrystals for quantum dot light-emitting diodes," RSC Adv. **7**, 10391–10396 (2017).
6. J. Shamsi, Z. Dang, P. Bianchini, C. Canale, F. Di Stasio, R. Brescia, M. Prato, and L. Manna, "Colloidal synthesis of quantum confined single crystal $CsPbBr_3$ nanosheets with lateral size control up to the micrometer range," J. Am. Chem. Soc. **138**, 7240–7243 (2016).
7. S. Sun, D. Yuan, Y. Xu, A. Wang, and Z. Deng, "Ligand-mediated synthesis of shape-controlled cesium lead halide perovskite nanocrystals via reprecipitation process at room temperature," ACS Nano **10**, 3648–3657 (2016).
8. A. Pan, B. He, X. Fan, Z. Liu, J. J. Urban, A. P. Alivisatos, L. He, and Y. Liu, "Insight into the ligand-mediated synthesis of colloidal $CsPbBr_3$ perovskite nanocrystals: The role of organic acid, base, and cesium precursors," ACS Nano **10**, 7943–7954 (2016).
9. V. K. Ravi, A. Swarnkar, R. Chakraborty, and A. Nag, "Excellent green but less impressive blue luminescence from $CsPbBr_3$ perovskite nanocubes and nanoplatelets," Nanotechnology **27**, 325708 (2016).
10. J. Li, X. Yuan, P. Jing, J. Li, M. Wei, J. Hua, J. Zhao, and L. Tian, "Temperature-dependent photoluminescence of inorganic perovskite nanocrystal films," RSC Adv. **6**, 78311–78316 (2016).
11. J. Butkus, P. Vashishtha, K. Chen, J. K. Gallaher, S. K. K. Prasad, D. Z. Metin, G. Laufersky, N. Gaston, J. E. Halpert, and J. M. Hodgkiss, "The evolution of quantum confinement in $CsPbBr_3$ perovskite nanocrystals," Chem. Mater. **29**, 3644–3652 (2017).
12. M. Jones, S. S. Lo, and G. D. Scholes, "Signatures of exciton dynamics and carrier trapping in the time-resolved photoluminescence of colloidal CdSe nanocrystals," The Journal of Physical Chemistry C **113**, 18632–18642 (2009).

#303952 https://doi.org/10.1364/OME.7.004367
Journal © 2017 Received 2 Aug 2017; revised 6 Oct 2017; accepted 10 Oct 2017; published 16 Nov 2017

Optical Materials EXPRESS

13. B. A. Koscher, J. K. Swabeck, N. D. Bronstein, and A. P. Alivisatos, "Essentially trap-free $CsPbBr_3$ colloidal nanocrystals by postsynthetic thiocyanate surface treatment," J. Am. Chem. Soc. **139**, 6566–6569 (2017).
14. F. Nanni, F. R. Lamastra, F. Franceschetti, F. Biccari, and I. Cacciotti, "Mo-doped indium oxide films by dip-coating: Synthesis, microstructure and optical properties," Ceramics International **40**, 1851–1858 (2014).
15. I. Gryczynski, J. Malicka, Z. Gryczynski, and J. R. Lakowicz, "Surface plasmon-coupled emission with gold films," J. Phys. Chem. B **108**, 12568–12574 (2004).
16. X. Huang and M. A. El-Sayed, "Gold nanoparticles: Optical properties and implementations in cancer diagnosis and photothermal therapy," J. Adv. Res. **1**, 13–28 (2010).
17. N. Dotti, F. Sarti, S. Bietti, A. Azarov, A. Kuznetsov, F. Biccari, A. Vinattieri, S. Sanguinetti, M. Abbarchi, and M. Gurioli, "Germanium-based quantum emitters towards a time-reordering entanglement scheme with degenerate exciton and biexciton states," Phys. Rev. B **91**, 205316 (2015).
18. H. He, Q. Yu, H. Li, J. Li, J. Si, Y. Jin, N. Wang, J. Wang, J. He, X. Wang, Y. Zhang, and Z. Ye, "Exciton localization in solution-processed organolead trihalide perovskites," Nature Communications **7**, 10896 (2016).
19. J. Li, L. Luo, H. Huang, C. Ma, Z. Ye, J. Zeng, and H. He, "2D behaviors of excitons in cesium lead halide perovskite nanoplatelets," J. Phys. Chem. Lett. **8**, 1161–1168 (2017).
20. F. Biccari, F. Gabelloni, E. Burzi, M. Gurioli, S. Pescetelli, A. Agresti, A. E. D. R. Castillo, A. Ansaldo, E. Kymakis, F. Bonaccorso, A. D. Carlo, and A. Vinattieri, "Graphene-based electron transport layers in perovskite solar cells: A step-up for an efficient carrier collection," Adv. Energy Mater. p. 1701349 (2017).
21. A. F. van Driel, G. Allan, C. Delerue, P. Lodahl, W. L. Vos, and D. Vanmaekelbergh, "Frequency-dependent spontaneous emission rate from CdSe and CdTe nanocrystals: Influence of dark states," Phys. Rev. Lett. **95**, 236804 (2005).
22. K. Gong, Y. Zeng, and D. F. Kelley, "Extinction coefficients, oscillator strengths, and radiative lifetimes of CdSe, CdTe, and CdTe/CdSe nanocrystals," J. Phys. Chem. C **117**, 20268–20279 (2013).
23. C. de Mello Donegá, M. Bode, and A. Meijerink, "Size- and temperature-dependence of exciton lifetimes in CdSe quantum dots," Phys. Rev. B **74**, 085320 (2006).
24. M. I. Dar, G. Jacopin, S. Meloni, A. Mattoni, N. Arora, A. Boziki, S. M. Zakeeruddin, U. Rothlisberger, and M. Grätzel, "Origin of unusual bandgap shift and dual emission in organic-inorganic lead halide perovskites," Sci. Adv. **2**, e1601156 (2016).
25. S. T. Birkhold, E. Zimmermann, T. Kollek, D. Wurmbrand, S. Polarz, and L. Schmidt-Mende, "Impact of crystal surface on photoexcited states in organic-inorganic perovskites," Adv. Funct. Mater. **27**, 1604995 (2017).

1. Introduction

All-inorganic metal halide perovskites have attracted a lot of attention in the last years in view of a novel class of optoelectronic devices [1–3]. In fact, this class of materials represents a very promising alternative to organo-metal halide perovskites, given their better long-term stability [4] and impressive radiative efficiency [5]. Therefore, all-inorganic metal halide perovskites are extremely attractive not only for photovoltaic cells but also for manufacturing efficient LEDs and lasers allowing to cover a spectral range from near ultra-violet to near-infrared depending on the halide composition [3].

An enormous research effort in the last decade has been devoted to the definition of growth and synthesis protocols [6–8] of all-inorganic metal halide perovskites with a control of the morphology and crystal size. In fact, depending on the specific application, different crystal sizes are necessary: from nanocrystals (NCs), in particular quantum dots (QDs), to crystals up to several hundreds of micrometers or even larger. Most of the reports consider ordered or disordered films of QDs, where the relationship between the photoluminescence (PL) emission energy and the QD size [9–11] is a clear evidence of quantum confinement effects.

It is worth noting that perovskite QDs are in principle remarkably different from III-V QDs (e.g. GaAs or InAs QDs), not only because of the more difficult control of the dot size in the chemical synthesis with respect to the epitaxial growth, but also because the absence of a wetting layer and semiconductor barriers make the perovskite QDs more similar to colloidal QDs (CQDs). In CQDs the nature of the dot surface plays a major role in the carrier dynamics [12] and therefore we expect the same behavior in our systems. In particular, we expect that surface states act as efficient centers for the capture of carriers, which can be released by thermal activation. Indeed, controlled modification of the dot surface, realized for instance with a metallic deposition on the perovskite film or a chemical treatment [13], can give rise to significant modification of the

Optical Materials EXPRESS

carrier trapping/detrapping processes by the surface. Nevertheless, concerning the time evolution of the PL signal, most of the results in the literature refer only to room-temperature data [7, 9]. Of course, this is relevant in view of the realization of optoelectronic devices, but provides incomplete information in presence of mechanisms that can be thermally activated.

In this contribution, by means of picosecond time-resolved photoluminescence (TR-PL) spectroscopy, we present an experimental study of the carrier recombination dynamics in a thin film of $CsPbBr_3$. We report a significant increase of the PL decay time as the temperature raises from 10 to 300 K. In particular, this effect is larger for the emissions at high energy, originating from carrier recombination in NCs, as already observed in CQDs [12]. The experimental results are interpreted considering a transfer of population from non-radiative surface trap states to radiative bulk states by a detrapping through a thermally activated mechanism similar to thermionic emission.

2. Experimental details

2.1. Synthesis of the sample

$CsPbBr_3$ was prepared following the synthesis protocol of Protesescu et al. [3]. Caesium carbonate (Cs_2CO_3, 0.1 g) was loaded into 100 mL two-neck flask along with octadecene (ODE, 30 mL) and oleic acid (OA, 2.5 mL), dried for 1 h at 120 °C, and then heated under N_2 flux to 150 °C until all Cs_2CO_3 reacted with OA. ODE (5 mL) and $PbBr_2$ (0.069 g) were loaded into 25 mL two-neck flask and dried under vacuum for 1 h at 120 °C. Dried oleylamine (OLA, 0.5 ml) and dried OA (0.5 mL) were injected at 120 °C under N_2 flux. After complete solubilization of a $PbBr_2$ salt, the temperature was raised to 150 °C for tuning the NCs size. Cs-oleate solution (0.4 mL in ODE, prepared as described above) was pre-heated to 100 °C and then quickly injected. The obtained suspension was centrifuged, and the supernatant removed. Then, the precipitate was washed with toluene and re-centrifuged another time. The new precipitate was dispersed in toluene forming long-term colloidal stable dispersions and deposited by drop-cast on a glass substrate. We have performed XRD analysis (not reported) which indicates only small traces of spurious phases (CsBr and $PbBr_2$) while the $CsPbBr_3$ orthorhombic phase dominates. Finally, $CsPbBr_3$ was covered by a metallic deposition of Pd/Au of about 10 nm to avoid the interaction with the environment. We chose Pd/Au as encapsulating layer instead of the common used Poly(methyl methacrylate) (PMMA) since we aimed to realize an half cavity to investigate the high excitation regime (data not presented in this paper), where amplified stimulated emission could be eventually observed.

2.2. PL characterization

PL experiments were performed in a quasi backscattering geometry, exciting and detecting from the Au side, keeping the sample in a closed cycle cryostat, varying the temperature in the range 10 - 300 K. Continuous wave (CW) measurements were performed using for excitation a laser diode operating at 3.06 eV with an excitation intensity of about 10 W/cm^2, while a frequency-doubled mode-locked ps Ti-Sapphire laser, operating at 81.3 MHz repetition rate with 1.2 ps pulses, was used for TR-PL experiments. The PL signal was spectrally dispersed by a 50 cm monochromator equipped with a 600 gr/mm (spectral resolution of 1 meV) and detected by a Charge Coupled Device detector (CCD) for CW PL spectra. TR-PL measurements were carried out using a time-correlated single photon counting technique (TCSPC) with a temporal resolution of about 60 ps, provided by an avalanche photodiode (APD).

3. Results and discussion

In Fig. 1(a) typical PL spectra of different regions (laser spot $\approx$ 100 µm diameter) of the sample are compared: multiple bands are observed. Given the intrinsic inhomogeneity of the drop-cast

Optical Materials EXPRESS

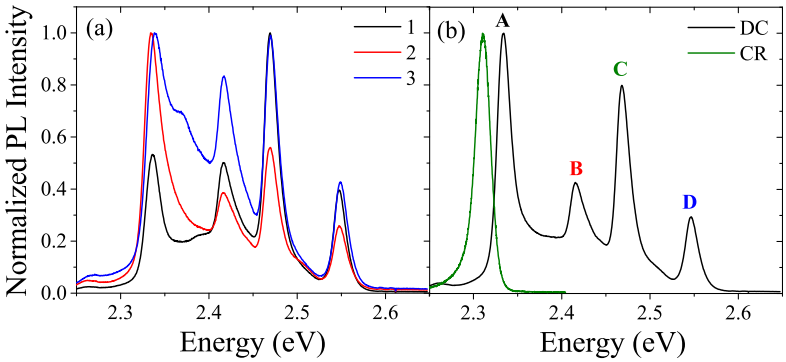

Fig. 1. (a) Normalized PL spectra at $T = 11$ K in different regions of the sample (1, 2, 3) after CW excitation at 3.06 eV. (b) Comparison between a normalized PL spectra of the sample (DC) and a normalized PL spectra of a bulk $CsPbBr_3$ crystal (CR).

deposition [14], the relative weight of each band changes when the excitation spot is moved on the sample over an area of a few mm^2. These bands can be ascribed only to PL emission of $CsPbBr_3$, since, as shown by XRD analysis the presence of CsBr and $PbBr_2$ is negligible and in any case their band gaps are much higher than $CsPbBr_3$. Moreover, we can also exclude that the observed bands originate from Au plasmon resonance: this resonance is expected at about 2.15 eV for Au films [15, 16], at lower energies with respect to the PL emissions of our sample (> 2.3 eV), and indeed a small broad band was observed at about 2.2 eV in our PL near field spectra (not shown). The linear dependence of the spectrally integrated PL intensity of each band on the excitation intensity (not shown) indicates that the radiative recombination arises from excitons [17] in agreement with previous reports [18, 19].

The comparison reported in Fig. 1(b) between the PL spectra of this sample (DC) and a 500 µm long $CsPbBr_3$ bulk crystal (CR) shows that the PL bands are all at higher energies with respect to bulk emission, therefore, since the presence of spurious phases can be neglected, we can assume that these bands originate from quantum confinement of excitons in NCs [6, 9–11]. Modeling our NCs as cubic QDs surrounded by an infinite potential barrier for the carriers, we can estimate the NCs size from the confinement energy, obtained from the difference between the emission energy of the PL bands and that of the bulk crystal (CR), taking into account the exciton binding energy. Even though, to our knowledge, the values of the static dielectric constant and of the effective masses of $CsPbBr_3$ are not univocally assigned, using the values calculated by Protesescu et al. [3], we estimate QD size of 16, 10, 9.0 and 7.5 nm for the bands A, B, C and D, respectively.

In Fig. 2(a) typical PL decays at the peak energy of each band are reported. The signal cannot be reproduced by a single exponential, as usually observed in $CsPbBr_3$ NCs with a distribution of traps and where the slow decay component is related to the trap dynamics [13]. Moreover, there is a clear slowing down of the PL time evolution when the energy decreases, i.e. increasing the size of the crystal. Fitting the experimental data with a two exponential function (dashed lines in Fig. 2(a)) and taking into account the laser pulse repetition rate [20], we can extract the radiative rate value Γ, corresponding to the initial fast decay. Results are shown in Fig. 2(b) and a deviation from linearity is evident for the highest energy band at 2.55 eV. As regard the slow relaxation time, it is about 5 ns for all emission bands and its weight is more important for the larger NCs.

In the strong confinement regime Γ is expected to linearly vary with QDs' size only because emission energy is changing [21], being the matrix element constant. In our case the expected variation of Γ is much smaller than the experimental observation in Fig. 2(b). CQDs show a PL time evolution very similar to the one here reported [22], which can be explained in terms of the thermal population of exciton dark states [21, 23] or invoking the contribution of surface state

Optical Materials EXPRESS

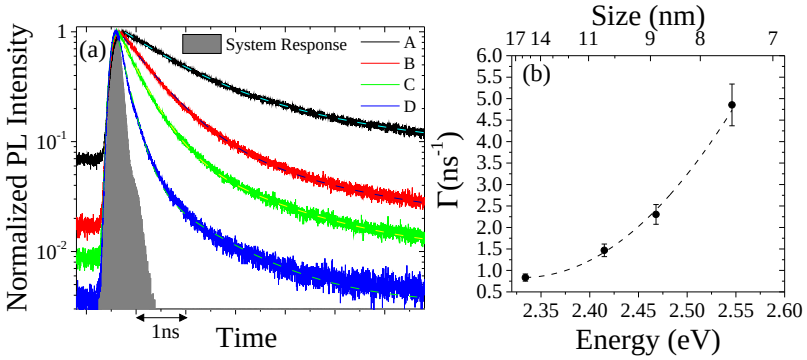

Fig. 2. (a) PL decay at $T = 11$ K for the different bands of Fig. 1(b) after ps excitation at 3.35 eV. The dashed lines are fits of the experimental data according to Ref. [20]. (b) Radiative rate as a function of the emission energy extracted from the PL decay of Fig. 2(a). The dotted line is a guide for the eye.

population [12]. In both cases the population in the dark or surface states acts as a reservoir for the radiative states and a significant slowing down of the PL time evolution is found increasing the temperature. It has to be noted that dark states are always in thermal equilibrium with radiative states while this is not true for surface states, given the presence of the potential barrier due to the surface. Therefore in presence of only dark states the PL decay should be monoexponential [21]. As a consequence, it is reasonable to assume the change of Γ mainly comes from the presence of trap states.

In order to confirm this interpretation we performed temperature dependent measurements. In Fig. 3(a-c) typical spectra are reported for three different temperatures, that show, with increasing temperature, a broadening of the emission and a blue shift for all the bands, typical of perovskite materials [10, 24]. It is worth noting that the ratio between the PL peak intensities changes with temperature: this indicates a lack of transfer of population between the different NCs. Moreover the spectral broadening is different for the various bands. These results confirm that the PL emission bands come from different structures.

In Fig. 3(d-g) the PL decays are reported for each band, as a function of temperature. For each temperature, PL decays were measured at the PL peak, taking into account the variation in the emission energy. An overall slow down of the decay is observed for each emission passing from 10 K to 300 K and, as a consequence, the pedestal P [20] observed before the PL rise increases with respect to the PL intensity at the peak decay. In particular, this effect is more relevant for the high energy emission bands (C, D) (see Fig. 3(f) and Fig. 3(g)). Given our experimental condition, where a ps laser pulse excites the sample every 12.3 ns, being the longest decay time constant of the order of several ns, the pedestal intensity can be considered as an estimate, through a constant of proportionality, of the stationary population in the radiative states.

In presence of a population in non-radiative states which can be transferred to the radiative states through a potential barrier, a slowing down of the PL decay is expected increasing the temperature. This result is not in contrast with the decrease of the spectrally integrated PL with the increase of temperature, since this reduction originates from a reduced number of photogenerated carriers into the radiative states. Given the morphology of the perovskites crystals, the origin of the non-radiative states acting as a sink for the radiative states can be ascribed to the NCs surface and their role is expected to be more relevant for smaller dots, since the ratio between the volume and the surface density of states scales with the dot size. As reported in CQDs [12], surface states can efficiently trap electrons and holes and therefore CQD surface is typically passivated to control the trap states [13, 25].

Optical Materials EXPRESS

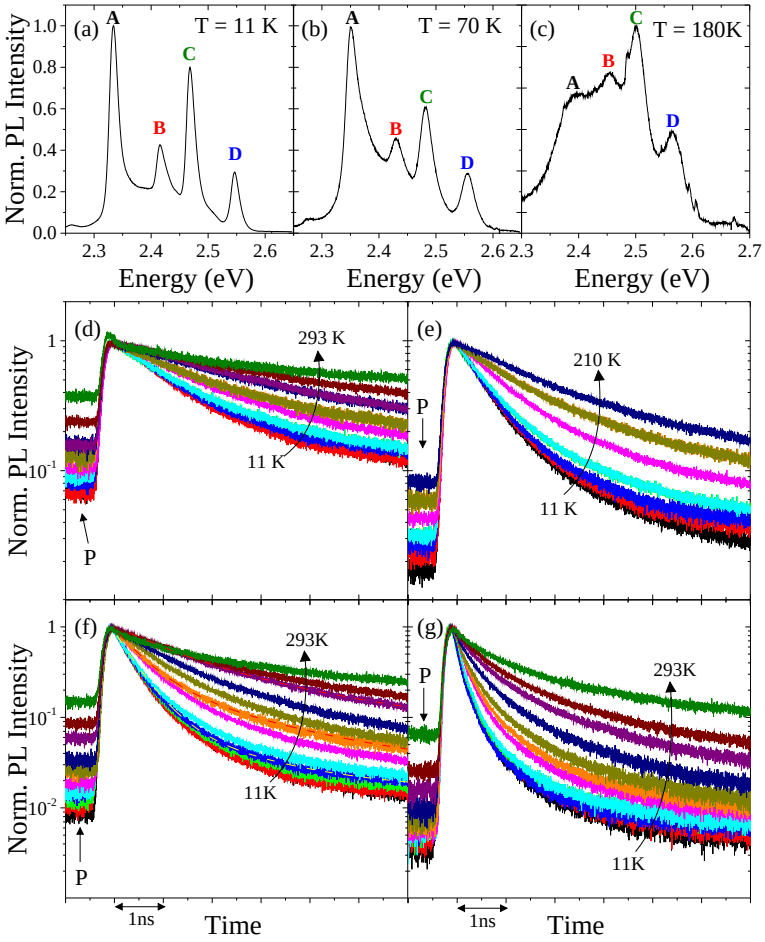

Fig. 3. (a-c) Normalized PL spectra at 11 K (a), 70 K (b) and 180 K (c). (d-g) PL decay as a function of the temperature for the band A (d), B (e), C (f) and D (g). Examples of fit according to Ref. [20] are shown as dashed lines in (f).

To take into account the transfer of population from the surface states back to the radiative states, we model the dependence of the pedestal P on the temperature T, according to the following equation:

$$P = \alpha T + \beta T^2 e^{-E_B/(k_B T)}, \quad (1)$$

In Eq. (1) α and β are two constants. The first term accounts for a phonon activated process, while the second term accounts for a thermally activated transfer of carriers, similar to a thermionic emission, from the surface states to the radiative states with an energy barrier E_B. In Fig. 4, for each band, the experimental data of P, normalized at the value measured at 10 K (P_0), are fitted according to Eq. (1). It turns out that, passing from band D to A, E_B reduces from 120 meV to 33 meV and the parameter β decreases of about two order of magnitude. Instead, α remains constant for the different bands. These results indicate that the presence of the barrier plays a major role for smaller NCs, as expected since their higher emission energies, and that at room temperature a thermal equilibrium between the surface and the bulk radiative states is possible only for the larger crystals.

Optical Materials EXPRESS

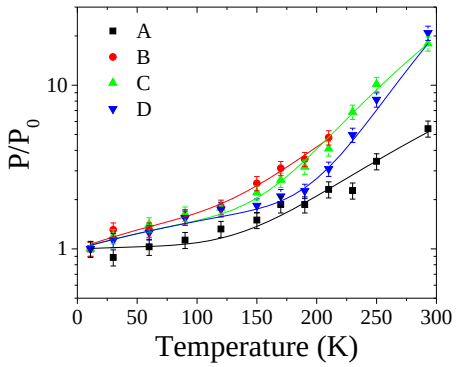

Fig. 4. Temperature dependence of the pedestal P, normalized to the value of P at 10 K (P_0), for each band: the continuous lines are the fits according to the Eq. (1).

4. Conclusions

In this work we have shown that the exciton recombination dynamics in $CsPbBr_3$ NCs is ruled by the carrier population and transfer from the surface states. This process accounts for the observed increase of the PL lifetime in NCs of different size. Estimate of the barrier height at the surface is provided considering a thermally activated mechanism similar to a thermionic emission for the release of carriers from the traps.

Funding

Ente Cassa di Risparmio (Firenze) (2015.1004, 2015.0937).

Acknowledgments

We warmly acknowledge Prof. F. Bogani for helpful discussions.